HHS Public Access

Author manuscript

Behav Res Ther. Author manuscript; available in PMC 2021 December 07.

Published in final edited form as:

Behav Res Ther. 2020 September ; 132: 103657. doi:10.1016/j.brat.2020.103657.

Neural mechanisms underlying heterogeneous expression of threat-related attention in social anxiety

Travis C. Evans[a,*], **Yair Bar-Haim**[b], **Nathan A. Fox**[c], **Daniel S. Pine**[d], **Jennifer C. Britton**[a,d,**]

[a]Department of Psychology, University of Miami, Coral Gables, FL, USA

[b]School of Psychological Sciences and Sagol School of Neurosciences, Tel Aviv University, Tel Aviv, Israel

[c]Department of Human Development and Quantitative Methodology, University of Maryland, College Park, MD, USA

[d]National Institute of Mental Health, Bethesda, MD, USA

Abstract

Theoretical frameworks propose that threat-related attention, which is typically assessed using the dot-probe paradigm, plays a key role in social anxiety. Within the dot-probe paradigm, novel computational approaches demonstrate that anxious individuals exhibit multiple patterns of threat-related attention on separate trials. However, no research has leveraged such novel computational methods to delineate the neural substrates of threat-related attention patterns in social anxiety. To address this issue, fifty-three socially anxious adults (22.38 ± 3.12, 33 females) completed an fMRI-based dot-probe paradigm. A novel, response-based computation approach revealed conjoint patterns of vigilant orientation, avoidant orientation, slow disengagement, and fast disengagement, which were masked by standard computation measures. Compared to vigilant orientation and fast disengagement, avoidant orientation and slow disengagement were greater in magnitude, respectively. Mirroring behavioral findings, avoidant orientation and slow disengagement elicited greater deactivation of several regions within the Default Mode Network and stronger connectivity between the right amygdala and superior temporal sulcus. Taken together, these results suggest that distinct neural processes facilitate the heterogeneous expression of threat-related attention in social anxiety.

Keywords

Attention; Information processing; Threat; Social anxiety; Neural; fMRI; Dot-probe

* Corresponding author. Department of Psychology, University of Miami, PO Box 248185, Miami, FL, 33124, USA., t.evans1@umiami.edu (T.C. Evans). ** Corresponding author. Department of Psychology, University of Miami, PO Box 248185, Miami, FL, 33124, USA., j.britton@miami.edu (J.C. Britton).

CRediT authorship contribution statement

Travis C. Evans: Conceptualization, Methodology, Software, Formal analysis, Writing - original draft, Visualization. **Yair Bar-Haim:** Conceptualization, Writing - review & editing. **Nathan A. Fox:** Conceptualization, Resources, Writing - review & editing, Supervision. **Daniel S. Pine:** Conceptualization, Resources, Writing - review & editing, Supervision, Funding acquisition. **Jennifer C. Britton:** Conceptualization, Methodology, Software, Formal analysis, Investigation, Resources, Data curation, Visualization, Supervision, Project administration, Writing - review & editing.

Declaration of competing interest

The study authors report no conflicts of interest.

1. Introduction

Perturbations in threat-related attention play a key role in the etiology and maintenance of social anxiety (Bar-Haim, Lamy, Pergamin, Bakermans-Kranenburg, & van IJzendoorn, 2007; Heeren, Mogoase, Philippot, & McNally, 2015). Across separate studies, however, individuals with social anxiety exhibit multiple expressions of threat-related attention. For example, socially anxious individuals may disproportionately orient attention towards or away from threat, or have difficulty disengaging attention from threat (e.g., Amir, Elias, Klumpp, & Przeworski, 2003; Klumpp & Amir, 2009; Mansell, Clark, Ehlers, & Chen, 1999; Pineles & Mineka, 2005). Given that different expressions of threat-related attention are putatively supported by distinct neurocognitive processes (Cisler & Koster, 2010), mechanistic insights into social anxiety are currently limited. Mixed findings may be attributable to standard computation approaches, which assume that threat-related attention is expressed in a consistent manner across trials. In contrast, novel computation methods demonstrate that anxious individuals may exhibit multiple, distinct patterns of threat-related attention across separate trials (Zvielli, Bernstein, & Koster, 2014a; 2014b). For example, an anxious individual may orient attention toward threat on some trials, but orient attention away from threat on other trials. The conjoint expression of both orientation patterns would suggest a more complex pattern of threat-related attention mechanisms in social anxiety (Evans & Britton, 2018). To systematically investigate the expression of threat-related attention and its neural mechanisms in social anxiety, the present study used both standard and novel dot-probe computation approaches in conjunction with fMRI methodology.

Meta-analytic findings demonstrate that social anxiety is characterized by an attentional bias in response to threat (Bar-Haim et al., 2007). Traditionally, attention bias is assessed by presenting threat-neutral stimulus pairs and comparing average reaction time (RT) on trials where response probes replace a threat (congruent trials) or a neutral stimulus (incongruent trials). Faster RT to congruent trials than incongruent trials suggests a bias towards threat, whereas slower RT suggests a bias away from threat. However, theoretical frameworks propose that threat-related attention can be further segregated into distinct cognitive processes of orientation and disengagement of attention (Koster, Crombez, Verschuere, & De Houwer, 2004; Mogg & Bradley, 2016). Specifically, orientation refers to the initial allocation of attention towards a threat, whereas disengagement refers to the subsequent shifting of attention away from a threat (Amir et al., 2003). To disentangle these components of attention in the dot-probe paradigm, RT on neutral-neutral trials serves as a reference to generate separate measures of orientation (congruent trials) and disengagement (incongruent trials; Koster et al., 2004; but for limitations, see Clarke, MacLeod, & Guastella, 2013).

Within these orientation and disengagement components, expressions of threat-related attention may be further dissociated along fuzzy boundaries of automatic and regulatory processes (Barry, Vervliet, & Hermans, 2015). Attentional models propose that vigilant orientation facilitates rapid, automatic detection of threats (Bar-Haim et al., 2007). In contrast, avoidant orientation regulates negative affect elicited by threat by directing attention away from threats (Cisler & Koster, 2010). Fast disengagement from threat may operate to automatically shift attention away from threats and towards safety cues (Cisler

& Koster, 2010; Yiend et al., 2015). Conversely, slow disengagement facilitates elaborative processing of threats and may stem from poor regulatory attentional processes (Cisler & Koster, 2010). In summary, these dissociable components of attention may be supported by related, but distinct, processes that are dysregulated in social anxiety.

Given these functional differences, distinct neural mechanisms are proposed to underlie each expression of threat-related attention (Cisler & Koster, 2010). Within the orientation component, the amygdala plays a central role in orienting attention towards threat (i.e., vigilant orientation; Monk et al., 2008; van den Heuvel et al., 2005). Conversely, avoidant orientation away from threat down-regulates amygdala activity by recruiting regulatory regions such as the ventrolateral prefrontal cortex (vlPFC; Adenauer et al., 2010; Browning, Holmes, Murphy, Goodwin, & Harmer, 2010; Fani et al., 2012; Kim & Hamann, 2007; Taylor et al., 2014). Within the disengagement component, fast disengagement is associated with less amygdala activation, which could be attributable to enhanced processing of non-threating stimuli (El Khoury-Malhame et al., 2011). Slow disengagement may reflect a failure to recruit the vlPFC, which impairs shifting attention away from threat (Bishop, 2009; Britton et al., 2012). Given these functional differences among components of attention, past research has aimed to more precisely characterize patterns of threat-related attention in social anxiety.

Across studies, however, social anxiety-related differences in orientation and disengagement components of attention are highly inconsistent. In separate samples, social anxiety has been associated with vigilant orientation, avoidant orientation, slow disengagement, or no differences in threat-related attention (e.g., Amir et al., 2003; Evans, Walukevich, & Britton, 2016; Klumpp & Amir, 2009; Mansell et al., 1999; Pineles & Mineka, 2005). Although some methodological differences exist across studies that may explain these divergent results, inconsistent findings are observed even when studies utilize similar or identical task parameters (Klumpp & Amir, 2009; Price, Tone, & Anderson, 2011; Vassilopoulos, 2005). As a result, it is unlikely that heterogenous findings in social anxiety can be attributed to methodological differences across studies. Instead, inconsistent findings may be attributable to the limitations of standard computation approaches, which characterize the direction in which attention is *generally* modulated by threat stimuli.

Recent research suggests that anxious individuals may express multiple patterns of threat-related attention, rather than a single, consistent pattern of threat-related attention (Zvielli et al., 2014a; 2014b). On separate trials, for example, an individual may orient attention towards threat or orient attention away from threat in equal magnitude (see Fig. 1). Because the magnitude of vigilant ($RT_{Neutral} > RT_{Congruent}$ = positive score) and avoidant trials ($RT_{Neutral} < RT_{Congruent}$ = negative score) average to form a zero score, this attention pattern would be miscategorized as a *general* absence of threat-related orientation. Additionally, individuals may exhibit vigilant and avoidant orientation on separate trials, albeit with unequal magnitudes (vigilant > avoidant = positive score). In both cases, a single average measure may obscure the conjoint presence of both vigilant and avoidant orientation in social anxiety. Similarly, a standard computation approach is also used in fMRI research employing the dot-probe paradigm to quantify neural activation patterns associated with threat-related attention. As a result, standard computation approaches that average neural

activation across trials may similarly fail to isolate neural mechanisms underlying each expression of threat-related attention.

To address these limitations, recent research has developed computation approaches that aggregate individual trials based on the type of threat-related attention exhibited on each trial (Evans & Britton, 2018; Zvielli et al., 2014a, 2014b). Using response-based computation, for example, individual reaction times on congruent trials can be *separately* indexed against that participant's *average* reaction time on neutral trials (i.e., Trial 1: $RT_{NeutralMean}$ - $RT_{Congruent\ 1,}$ Trial 2: $RT_{NeutralMean}$ - $RT_{Congruent\ 2}$ … Trial *n*: $RT_{NeutralMean}$ - $RT_{Congruent\ n}$). Across trials, positive and negative difference scores are subsequently aggregated to generate separate measures of vigilant orientation and avoidant orientation, respectively (see Fig. 1). Consistent with capturing distinct attention processes, response-based computation improves psychometric properties of threat-related attention measures and reveals unique anxiety-related associations (Evans & Britton, 2018).

By isolating specific attention processes using response-based computation, it is possible to address several related research questions concerning social anxiety. First, heterogeneous expressions of threat-related attention in social anxiety are consistent with mixed findings observed across previous studies. Dissociating attentional processes across trials may more accurately characterize threat-related attention in social anxiety. For example, social anxiety may not be characterized by one particular pattern of threat-related attention (e.g., vigilant orientation), but instead be more accurately characterized by multiple expressions of threat-related attention across trials (vigilant orientation *and* avoidant orientation). Second, dissociating attentional processes across trials may better isolate the neural mechanisms that contribute to conjoint patterns of threat-related attention in social anxiety. Specifically, evoked neural signatures can be directly extracted from trials in which a particular expression of threat-related attention is observed. Finally, the behavioral and neural measures generated by response-based computation may reveal anxiety-related associations that provide additional mechanistic insights into social anxiety. To date, however, no research has utilized response-based computation in conjunction with fMRI methodology in a socially anxious sample.

To address these research questions, we utilized standard and novel dot-probe computation approaches in conjunction with fMRI data from a previously published attention training study (Britton et al., 2015). In this previous report, the authors characterized neural activation changes associated with Attention Bias Modification (ABM) training in a sub-clinical social anxiety sample. Prior to randomization to active ABM or placebo protocols, participants completed the same baseline dot-probe task while in the MRI scanner (Amir et al., 2009). In the published study, ABM-related changes in neural activation were examined in a smaller sub-sample of individuals who completed all treatment phases ($n = 30$). In the current study, we analyze data from the larger baseline sample who completed the baseline dot-probe task in the MRI scanner prior to treatment randomization ($n = 53$).

Using response-based computation in this larger baseline sample, we hypothesized that social anxiety would be characterized by the conjoint presence of multiple threat-related attention patterns (i.e., vigilant orientation, avoidant orientation, and slow disengagement),

which would not be observed in standard computation measures. Based on previous conceptualizations and empirical research (Bishop, 2009; Browning et al., 2010; Cisler & Koster, 2010; Monk et al., 2008; Taylor et al., 2014), we hypothesized that each pattern of threat-related attention would be associated with distinct neural signatures. First, we hypothesized that vigilant orientation would be characterized by greater amygdala activation, whereas avoidant orientation would be characterized by greater connectivity between the amygdala and vlPFC. Second, we hypothesized that and faster and slower disengagement from threat would be characterized by stronger and weaker vlPFC activation, respectively.

2. Methods

2.1. Participants

Through collaboration between the University of Maryland and the National Institute of Mental Health (NIMH), fifty-three adults reporting sub-clinical levels of social anxiety were recruited (33 females; age range: 18–30 years old; M = 22.38 years old, SD = 3.12). Specifically, participants were initially recruited based on reporting a score greater than 50 on the Liebowitz Social Anxiety Scale (LSAS; Liebowitz, 1987), which approximates symptom levels observed in Social Anxiety Disorder (SAD; Rytwinski et al., 2009). At the time of the baseline scan session, the majority of participants (82%) continued to self-report clinically elevated levels of social anxiety on the LSAS (M = 42.94, SD = 20.58; Baker, Heinrichs, Kim, & Hofmann, 2002). Based on the Structured Clinical Interview for DSM-IV (First, Spitzer, Gibbon, & Williams, 2002), all participants were free of any current Axis I disorders. Participants were required to exhibit an IQ score greater than 70 based on the Wechsler Abbreviated Scale of Intelligence Vocabulary and Matrix Reasoning subtests (Wechsler, 1999). All participants were free of psychotropic medication, significant medical issues, and MRI contraindications.

From this larger sample (n = 53), 3 participants were ultimately excluded due to accuracy levels below 70% on the baseline dot-probe task (n = 2) or fMRI signal artifact during the task scan (n = 1). Using non-parametric tests due to the small number of excluded participants, these groups did not differ in gender, age, IQ, depressive symptoms, or social anxiety symptoms (all p's > 0.11). Following these exclusions, all analyses were conducted in a final sample of 50 participants (30 females; M = 22.01 years old, SD = 2.85).

2.2. Procedure

Following screening procedures, participants completed several MRI scans at the National Institute of Mental Health NIMH). While in the MRI scanner, participants completed a baseline dot-probe task, which has been used in previous social anxiety research (Amir et al., 2009). After completing the baseline MRI scan, participants received either ABM or placebo attention training protocols based on random assignment and returned for a follow-up scan (Britton et al., 2015). In the current study, we analyzed data from the baseline fMRI session that were collected from all participants prior to receiving active or placebo attention training (n = 53).

2.3. Measures

2.3.1. Liebowitz social anxiety scale (LSAS)—The LSAS is a 24-item scale that measures the level of fear and avoidance an individual demonstrates during several types of social situations (Liebowitz, 1987). For each social situation (e.g., talking on the telephone in public), participants report how much fear was experienced (0 = None; 3 = Severe) and how often the situation was avoided (0 = Never; 3 = Usually) during the previous week. The total composite social anxiety score includes both fear and avoidance scales, with total scores ranging between 0 and 144. As a measure, the LSAS demonstrates excellent internal consistency (Cronbach's a = 0.96; Heimberg et al., 1999). Additionally, the LSAS demonstrates good test-retest reliability (0.83) across a 12 week period (Baker et al., 2002).

2.3.2. The Beck depression Inventory-II (BDI-II)—The BDI-II measures the intensity of various depression symptoms experienced over a two week period (Beck, Steer, & Brown, 1996). The BDI-II is a 21-item scale (e.g. 0 = I do not feel sad; 3 = I am so sad or unhappy that I can't stand it) that yields a total composite score between 0 and 63. The BDI-II demonstrates excellent internal consistency as well as an excellent test-retest reliability of 0.93 over a period of 1 week (Beck et al., 1996).

2.4. Dot-probe task

The dot-probe task was programmed and presented using E-Prime 2.0 software (Pittsburgh, PA). On dot-probe task trials, participants viewed a fixation cross at the center of the screen. Next, two facial expressions of the same individual were presented simultaneously above and below the fixation cross. Face pairs were either an angry and neutral face or two neutral faces. For angry-neutral face pairs (threat trial), the angry face was equally likely to appear above or below the fixation. After the faces disappeared from the screen, a response probe ("E" or "F") replaced one of the locations previously occupied by a face. The response probe randomly replaced the angry (congruent trial) or neutral (incongruent trial) face at equal frequencies. For neutral face pairs (neutral trial), the response probe randomly appeared above or below fixation with equal frequencies. Participants identified the response probe via button press as quickly and accurately as possible. In addition to task trials, presentation of fixation-only trials facilitated deconvolution of the hemodynamic signal.

In total, the dot-probe task consisted of 192 trials (48 congruent, 48 incongruent, 48 neutral, 48 fixation-only). On average, trials were 2500 ms long, with 500 ms fixation, 500 ms face pair, 400 ms probe and an average jittered inter-trial interval (ITI) of 1100 ms (Range: 900–1300 ms).

2.5. fMRI data acquisition

MRI data were collected using a 3.0T General Electric Signa system scanner (Waukesha, WA) with an eight-channel gradient head coil. For functional imaging, a T2*-sensitive gradient echo pulse sequence was used (TR = 2300 ms, TE = 25 ms, flip angle = 90°, FOV = 24 cm, 96 × 96 acquisition matrix, 36 contiguous 2.6 mm interleaved axial slices). The first four acquisition images were discarded to allow magnetization equilibrium prior to task onset. Following the task, a T1-weighted scan of the whole brain was acquired using a high-resolution gradient echo sequence (124.12 mm axial slices, FOV = 220 mm, NEX = 1,

256 × 192 acquisition matrix, TI = 725 ms). The anatomical scan was used to co-register and normalize functional imaging data.

2.6. Data reduction

2.6.1. Behavioral data—Prior to conducting analyses, behavioral data were inspected for accuracy and reaction time outliers. Participants with an accuracy rate lower than 70% were excluded from all analyses due to poor task performance ($n = 2$). In line with typical data cleaning procedures, incorrect responses were identified as error trials and excluded. Additionally, trials with reaction times less than 150 ms or greater than 2000 ms were removed. After accounting for errors and trials outside the expected RT range, individual condition-level outliers were identified and removed. For each participant, trials were excluded when reaction times deviated 2.5 SD from the mean RT within each condition.

2.6.2. Standard computation of orientation and disengagement—As noted previously, attention bias to threat may be attributable to *faster* reaction times on congruent trials (i.e., facilitated orientation towards threat) or *slower* reaction times on incongruent trials (i.e., difficulty disengaging from threat; Koster et al., 2004). To address this issue, congruent reaction times and incongruent reaction times are separately compared to neutral reaction times (Koster et al., 2004). By utilizing a neutral reference condition, attention bias can be decomposed to examine both orientation towards threat ($RT_{NeutralMean} - RT_{CongruentMean}$) and disengagement from threat ($RT_{IncongruentMean} - RT_{NeutralMean}$). For the orientation index, positive scores indicate vigilant orientation to threat, whereas negative scores indicate avoidant orientation. For the disengagement index, positive scores indicate slowed disengagement from threat; whereas, negative scores indicate faster disengagement from threat.

2.6.3. Standard computation of attention bias—Although our analyses focused on dissociating orientation and disengagement, we also computed behavioral measures of attention bias for completeness. Typically, attention bias is assessed by subtracting the average congruent reaction times from average incongruent reaction times (i.e., $RT_{IncongruentMean} - RT_{CongruentMean}$). Using this computation, positive scores indicate an attention bias towards threat, negative scores indicate an attention bias away from threat, and zero-level scores indicate a lack of attention bias.

2.6.4. Response-based computation of orientation and disengagement—Recently, novel computation methods were developed to overcome several limitations of standard computation approaches (Evans & Britton, 2018; Zvielli et al., 2014a, 2014b). To capture varying expression of threat-related attention across trials, for example, response-based computation compares individual trial reaction times to a mean reference reaction time. Specifically, response-based computation compares reaction times on each *individual* congruent or incongruent trial to the neutral reference condition to separately assess vigilant and avoidant orientation as well as slow and fast disengagement (Evans & Britton, 2018). To assess distinct patterns of orientation to threat, for example, each congruent trial reaction time is separately referenced against the mean RT of neutral trials (i.e., $RT_{NeutralMean} - RT_{Congruent\ [Trial1\ \ldots\ Trial2\ \ldots\ Trial\mathit{n}]}$). Following this computation approach, separate

distributions of vigilant (i.e., trials producing positive difference scores) and avoidant orientation (trials producing negative difference scores) are obtained. Following response-based categorization of individual trials, difference scores *within* each response category are subsequently averaged into separate measures. Within orientation to threat, for example, positive difference scores are identified and subsequently averaged to form a measure of vigilant orientation. Similarly, negative difference scores are identified and subsequently averaged to form a measure of avoidant orientation. The magnitude of these separate response-based measures indicates the degree to which an individual exhibits vigilant orientation and avoidant orientation. Similar methods can be applied to separate slower and faster patterns of disengagement from threat using incongruent trials (i.e., $RT_{Incongruent\ [Trial1 \ldots Trial2 \ldots Trial\mathit{n}]} - RT_{Neutral}$).

2.6.5. fMRI Data—Prior to analysis, fMRI data were preprocessed with typical procedures using Analysis of Functional NeuroImages (AFNI) software. First, EPI images were slice-time corrected and realigned to the first image of each time-series. Following these steps, the EPI image was co-registered to the anatomical image and subsequently normalized within Talairach space. Next, functional data were smoothed with a 6 mm full-width-at-half maximum isotropic Gaussian filter and converted to a percent signal change relative to baseline fixation trials. Finally, motion parameters were examined to identify participants who exhibited excessive head motion during the scan (> 3 mm translation or > 3° rotation across 75% of TRs). No participants were removed due to excessive motion. However, one participant was removed due to a technical issue that produced an extensive fMRI signal artifact in the occipital cortex.

Following preprocessing procedures, we generated two sets of first-level models according to standard and response-based computation methods. For standard computation, individual models were generated according to task-defined conditions. Specifically, congruent, incongruent, and neutral trials were convolved with a gamma variate function to approximate the hemodynamic response. Finally, excluded trials were modelled as a separate regressor of no interest.

For the response-based computation methods, individual models were generated classifying each trial in reference to the participant's mean neutral reaction time (e.g., $RT_{NeutralMean} - RT_{Congruent\ [Trial1 \ldots Trial2 \ldots Trial\mathit{n}]}$; see Fig. 2). For individual congruent trials, positive responses were coded as vigilant orientation trials, whereas negative responses were coded as avoidant orientation trials. For incongruent trials, positive responses were coded as faster disengagement trials, whereas negative responses were coded as slower disengagement trials. Based on this approach, each individual model contained 5 regressors (i.e., vigilant orientation, avoidant orientation, slower disengagement, faster disengagement, or neutral trials). Regressors were formed by convolving stimulus onset times with a gamma function to approximate the hemodynamic response. For each response-based condition, we also computed a regressor in which amplitude was parametrically modulated by the RT of each individual trial. Given that no parametric modulation was observed by RT, these modulated task regressors are not discussed further. Similar to the standard model, we also modelled several covariates of no interest. Error trials, outlier trials, and trials demonstrating non-

directional responses (e.g., $RT_{NeutralMean} = RT_{Congruent\ [Trial\ n]}$) were modelled as a single error regressor.

For both standard and response-based models, identical six rigid-body motion regressors were derived for each individual to model motion translation and motion rotation in the xyz direction. Finally, regressors modelling both linear and non-linear low-frequency temporal drift in the scanner were included. Beta weights for all effects including error responses were estimated to maximize model fit.

2.7. Data analysis strategy

Behavioral measures.—For standard computation measures, we conducted separate one sample t-tests that compared average indices of orientation ($RT_{NeutralMean} - RT_{CongruentMean}$), disengagement ($RT_{IncongruentMean} - RT_{NeutralMean}$), and traditional attention bias ($RT_{IncongruentMean} - RT_{CongruentMean}$). Significant point estimates indicated that threat *generally* skewed orientation and/or disengagement of attention.

For response-based measures, a one-sample test analysis approach may inherently inflate the probability of obtaining non-zero results given the manner in which trials are sub-divided. As such, we focused on comparing the *relative* magnitude of response-based measures. To compare the relative magnitude of threat-related attention patterns, the absolute magnitude of response-based measures were then submitted to a 2 (Attention Type: Orientation vs. Disengagement) x 2 (Attention Direction: Positive (vigilant, slower disengagement) vs. Negative (avoidant, faster disengagement) Repeated Measures (RM)-ANOVA. For all behavioral analyses, statistical significance was determined at $a \leq 0.05$.

Neural activation.—For standard computation, we conducted an omnibus group-level model comparing task-defined conditions (i.e., congruent, incongruent and neutral condition means). For the response-based computation omnibus group-level model, we conducted a 2 (Attention Type: Orientation vs. Disengagement) x 2 (Attention Direction: Positive (vigilant, slow disengagement) vs. Negative (avoidant, fast disengagement). Both models employed random effects modelling utilizing AFNI 3dMVM. For both standard and response-based models, we conducted both region of interest analysis and whole-brain analysis. *A priori* seed regions were interrogated using anatomically defined regions or coordinates based on previous research. Separate left and right anatomical amygdala seeds were identified using the Talahraich-Daemon atlas in AFNI. The binarized amygdala masks were subsequently resampled to match the EPI data (2.5 mm isotropic voxels). Based on previous research suggesting that the ventrolateral prefrontal cortex (vlPFC) plays a central role in regulating threat-related attention, an 8 mm sphere was placed on the Talaraich analogue of the peak activation voxel [28, 21, 1] identified by Browning and colleagues (Browning et al., 2010).

For whole-brain analyses, family-wise error was controlled using a combined voxel-wise and cluster threshold approach. To obtain a cluster threshold using $\alpha = 0.05$, 10,000 Monte Carlo simulations were run using the recently developed non-parametric ClustSim function within AFNI (Cox, Chen, Glen, Reynolds, & Taylor, 2017). Based on initial voxel-wise threshold of $p = 0.005$ and the observed smoothness of estimated residuals (ACF parameters: 0.55, 4.76, 13.18), a 114-voxel (1781.25 mm^3) cluster level threshold corrected for multiple

comparisons at $p = 0.05$ across a whole-brain masked search territory. Peak activation voxel coordinates are reported within LPI reference space.

For the *a priori* seed and functionally defined regions, mean percent signal changes for each response-based condition were extracted using AFNI 3dROIstats. Following extraction, we conducted follow-up RM-ANOVAs in SPSS. For all neural analyses, statistical significance was determined at $a \leq 0.05$.

Neural connectivity.—In addition to analyses examining neural activation, we examined functional connectivity using both standard and response-based computation. Utilizing a generalized form of context-dependent psychophysiological interaction analyses (gPPI; McLaren, Ries, Xu, & Johnson, 2012), we examined how the *a priori* ROIs (bilateral anatomical amygdala and vlPFC) differed in functional connectivity with other neural regions as a function of standard (e.g., congruent) or response-based (e.g., vigilant orientation) task regressors.

To conduct gPPI analyses, we first computed interaction terms. These gPPI interaction terms represent the product of a neural seed time series and each task regressor. First, we extracted the time series of hemodynamic activity from an *a priori* seed region. Next, we deconvolved the time series with a gamma variate function to approximate the hemodynamic response function (HRF). We convolved the raw time series with the four response-based conditions (i.e., vigilant orientation, avoidant orientation, slowdisengagement, and fast disengagement) and neutral condition. As stimulus onset times were desynchronized with TR acquisition, we up-sampled neural time series and task regressors before computing gPPI regressors. After computing gPPI regressors, gPPI interaction terms were down sampled to the original acquisition sampling rate. Finally, the gPPI interaction regressors were convolved with a gamma function approximating the HRF.

Individual gPPI models included terms representing the interaction between the seed time series and the response-based conditions as well as parameters of the original model. For both standard and response-based models, we included the original task regressors, the same motion parameters, scanner drift parameters, and single error regressor specified in our neural activation analyses. Similar whole-brain analyses were conducted using the gPPI interaction coefficients rather than percent signal change values.

Anxiety-Related Associations.—In the absence of a non-anxious control group, we examined anxiety-related associations within our sample. To test which behavioral and neural threat-related attention patterns are *distinctly* associated with social anxiety, we compared anxiety-related associations between response-based conditions. Past behavioral research suggests that greater vigilant orientation, relative to avoidant orientation is associated with anxiety levels (Evans & Britton, 2018). As such, we separately compared social anxiety-related associations among response-based conditions within the orientation (vigilant vs. avoidant) and disengagement (fast vs. slow) components. In addition to behavioral measures, we focused anxiety-related analyses on neural regions that exhibited response-based differences in neural activation or neural connectivity to minimize the number of total analyses.

3. Results

3.1. Behavioral data

3.1.1. Standard computation—To test standard indices of orientation to threat ($RT_{NeutralMean} - RT_{CongruentMean}$) and disengagement from threat ($RT_{IncongruentMean} - RT_{NeutralMean}$), we utilized one-sample t-tests. Across the sample, analyses revealed no evidence of either skewed orientation to threat (M = 0.47 ms, SD = 21.09; $t(49)$ = 0.16, p = 0.88; 95% CI [−5.52, 6.46]) or skewed disengagement from threat (M = −0.05 ms, SD = 17.07; $t(49)$ =−0.02, p = 0.98; 95% CI [−4.90, 4.80]). Although not a primary aim of the current study, no evidence of attention bias was observed using traditional contrast scores ($RT_{IncongruentMean} - RT_{CongruentMean}$; M = 0.42 ms, SD = 20.19; $t(49)$ = 0.15, p = 0.89; 95% CI [−5.32, 6.16]).

3.1.2. Response-based computation—Comparing the absolute magnitude of response-based measures revealed a significant Attention Type × Attention Direction interaction ($F_{1, 49}$ = 9.19, p = 0.004; η_p^2 = 0.16; 95% CI [−21.57, −4.37]; see Fig. 3). Within the orientation component, avoidant orientation (M = 68.93 ms, SD = 26.91 ms) was greater in absolute magnitude compared to vigilant orientation (M = 61.27 ms, SD = 24.42 ms; $F_{1, 49}$ = 7.91, p = 0.007; η_p^2 = 0.14; 95% CI [−13.13, −2.19]). Within the disengagement component, slow disengagement (M = 68.01 ms, SD = 25.46 ms) was marginally greater in absolute magnitude compared to fast disengagement (M = 62.69 ms, SD = 23.71 ms; $F_{1, 49}$ = 3.913, p = 0.05; η_p^2 = 0.07; 95% CI [−0.07, 10.69]).

Post-Hoc Analyses (Frequency).: Given response-based differences in magnitude, it is notable that such differences were not detected in standard attention measures (e.g., $Neutral_{RT} - Congruent_{RT}$). In addition to relative *magnitude*, we also examined if there were relative differences in the *frequency* of response-based measures. For example, avoidant orientation may exhibit greater *magnitude* compared to vigilant orientation (e.g., avoidant = 30 ms; vigilant = 15 ms), but also occur relatively less *frequently* (e.g., avoidant = 10 trials; vigilant = 20 trials). Due to the equal weighting of trials by standard attention measures, however, response-based differences in magnitude would be effectively masked.

To test this possibility, we compared the relative *frequency* of response-based measures. After confirming that the distributions of response types *frequencies* were each normally distributed with Shapiro-Wilk tests (all p's > 0.14), we submitted the frequency of response-based measures to a 2 (Attention Type) × 2 (Attention Direction) RM-ANOVA. Consistent with our *post-hoc* hypothesis, we observed differences in the relative *frequency* of response-based measures as evidenced by a significant Attention Type × Attention Direction interaction ($F_{1, 49}$ = 8.59, p = 0.005; η_p^2 = 0.15; 95% CI [1.82, 9.78]). We then conducted paired-samples t-tests within each attention component. Within the orientation component, avoidant orientation (M = 20.98 trials, SD = 4.89) were significantly less frequent compared to vigilant orientation (M = 24.42 trials, SD = 4.46; $t(49)$ = 2.68, p = 0.01). Within the disengagement component, slow disengagement (M = 21.32 trials, SD = 4.08) were significantly less frequent compared to fast disengagement (M = 23.68 trials, SD = 3.65; $t(49)$ = −2.37, p = 0.02).

Post-Hoc Analyses (Distribution Topography).: When averaged *across* subjects, mean RTs are not normally distributed, but instead exhibit a positive skew. However, it remains unclear if RTs exhibit a similar skew within *individual* subjects, which our response-based approach aims to characterize. If RTs exhibit a consistent positive skew at the *individual subject* level, our response-based results may simply be attributable to the topography of RT distributions, rather than distinct attentional processes. To test this possibility, we conducted additional post-hoc analyses.

First, we quantified the normality of RT distributions at the *individual subject* level using Kolmogorov-Smirnov tests of normality. For congruent trials, most subjects exhibited normal RT distributions (72%), whereas a minority of subjects exhibited either positively skewed RT distributions (18%) or negatively skewed RT distributions (10%; see Fig. 4). For incongruent trials, most subjects exhibited normal RT distributions (58%), whereas a minority of subjects exhibited either positively skewed RT distributions (18%) or negatively skewed RT distributions (24%; see Fig. 5). Based on these results and descriptive examination of Figs. 4 and 5, it seems unlikely that our response-based results are simply a topographical feature of RT distributions.

Second, we confirmed our response-based results using non-parametric analyses that are robust against violations of normality. Specifically, we utilized a Related-Samples Friedman's Two-Way Analysis of Variance by Ranks, which is more appropriate in cases in which distributions exhibit non-normality. This analysis essentially performs a non-parametric version of the previously reported 2 × 2 RM-ANOVA. Similar to our parametric results, we observed a significant 2 × 2 interaction ($p = 0.048$). We then used non-parametric Wilcoxon Ranked tests to conduct follow-up analyses. Similar to the original paired-samples t-tests, avoidant orientation was greater in absolute magnitude relative to vigilant orientation ($p = 0.01$) and slow disengagement was greater in absolute magnitude relative to fast disengagement ($p = 0.047$).

Third, it could be argued that response-based differences are attributable to slower and faster RT more generally. Compared to the neutral reference, slower RT on congruent and incongruent trials generate avoidant orientation and slower disengagement indices, respectively. Likewise, comparatively faster RT on congruent and incongruent trials generate vigilant orientation and faster disengagement. Given that the magnitude of avoidant orientation and slower disengagement was greater than the magnitude of vigilant orientation and faster disengagement, it is possible that individuals might simply respond comparatively more slowly on both congruent and incongruent trials. Similar to our observed pattern of response-based differences, this general slowing of RT would also produce a larger magnitude of avoidant orientation and slower disengagement (i.e., slow responses) relative to vigilant orientation and faster disengagement (i.e., fast responses).

Given that RT values of an individual will be highly correlated, we used difference scores to compare orientation (i.e., $RT_{Vigilant} - RT_{Avoidant}$) and disengagement (i.e., $RT_{Fast} - RT_{Slow}$) to rule out this possibility. First, we examined the correlation between each difference score and overall RT. Overall RT was not associated with either differences within orientation ($t(49) = 0.12$, $p = 0.43$) or disengagement indices ($t(49) = 0.21$, $p = 0.15$).

Second, we observed only a modest correlation between orientation difference scores and disengagement difference scores, ($t(49) = 0.26$, $p = 0.07$). Taken together, these results suggest that differences among orientation and disengagement response-based measures were not attributable to intra-individual variability in general reaction time.

3.2. Neural activation

3.2.1. Standard computation—When comparing congruent and incongruent task-defined conditions to neutral conditions, no significant differences in neural activation were detected using *a priori* amygdala or vlPFC seeds (all p's > 0.33).

3.2.2. Response-based computation—Similar to the condition-based approach, response-based computation did not yield differences in neural activation within the right amygdala, left amygdala, or vlPFC ROIs (all p's > 0.12).

However, three clusters survived whole-brain correction for the hypothesized two-way Attention Type × Attention Direction interaction. Specifically, we observed response-based differences in clusters containing the bilateral posterior cingulate cortex (PCC; [−28, −46, 24], 525 voxels (8203 mm^3); BA 31), the medial prefrontal cortex (mPFC; [−4, −59, 12], 126 voxels (1969 mm^3); BA 10), and the left superior frontal gyrus (lSFG; [−11, 51, 36], 118 voxels (1844 mm^3; see Fig. 6); BA 9).

Across all three clusters, we observed a similar pattern of activation differences among response types (see Fig. 6). Within the orientation component, we observed greater deactivation during avoidant orientation compared to vigilant orientation (all $p's < 0.007$; all 95% CI's [0.03, 0.19]) and during slow disengagement compared to fast disengagement (all $p's < 0.04$; all 95% CI's [−0.18, −0.005]). One-sample t-tests confirmed that avoidant orientation and slow disengagement were characterized by significant deactivation relative to baseline (all $p's < 0.01$; all 95% CI's [−0.21, −0.02]). In contrast, neural activation during vigilant orientation and fast disengagement did not differ from baseline (all $p's > 0.28$; all 95% CI's [−0.09, 0.03]).

Post-hoc neural coherence results.: Response-based computation revealed converging de-activation patterns *within* several neural regions (PCC, mPFC, and left SFG) that are putative hubs within the larger Default Mode Network (DMN; Greicius, Krasnow, Reiss, & Menon, 2003). To test this possibility, we tested if individual differences in neural activity within one region co-varied with the neural activity *across* the other two regions (e.g., *corr*(PCC-vigilant, mPFC-vigilant); *corr*(PCC-vigilant, SFG-vigilant), etc.). For each response-based condition, we utilized Pearson bivariate product-moment correlations to test coherence of neural activation across regions. All response-based conditions exhibited strong coherence of neural activity across the PCC, mPFC, and left SFG (average $r = 0.71$, average $p < 0.001$). Moreover, this pattern of coherence was largely absent across *different* response types (e.g., *corr*(PCC-vigilant, mPFC-avoidant) for both orientation (average $r = 0.08$, average $p = 0.61$) and disengagement (average $r = 0.24$, average $p = 0.12$). Although these analyses were exploratory in nature, this pattern of coherence suggests that response-based patterns of attention elicited divergent deactivation of DMN hubs.

3.3. Neural connectivity

3.3.1. Standard computation—Whole-brain analyses of functional connectivity using *a priori* seed regions failed to identify any neural clusters characterized by condition differences.

3.3.2. Response-based computation—For the right amygdala seed, we observed response-related differences in neural connectivity to a cluster extending across the right middle occipital cortex and posterior aspects of the right superior temporal sulcus (STS; [41, −49, 1], 294 voxels (4594 mm^3; see Fig. 7). Stronger connectivity between the right amygdala and this occipito-STS cluster was observed during avoidant orientation compared to vigilant orientation ($F_{1, 49} = 10.27$, $p = 0.002$; $\eta_p^2 = 0.17$; 95% CI [−0.79, −0.18]). Similarly, stronger connectivity between these regions was observed during slower disengagement compared to faster disengagement ($F_{1, 49} = 7.88$, $p = 0.007$; $\eta_p^2 = 0.14$; 95% CI [0.10, 0.58]). Of note, one sample t-tests demonstrated that all response-based conditions exhibited stronger amygdala-STS connectivity relative to baseline (gPPI Beta Coefficients: 0.49–0.97, all *t*'s > 4.31, all *p's* < 0.001; all 95% CI's [0.26, 1.32]).

When selecting the left amygdala and vlPFC as seed regions, however, no clusters survived whole brain corrected cluster threshold.

3.4. Anxiety-Related Associations

At the behavioral level, no standard or response-based measures were associated with social anxiety (all *p's* > 0.15) Across neural activation patterns within the PCC, mPFC, or left SFG, no significant anxiety-related interactions were observed for orientation or disengagement components (all *p's* > 0.08).

However, social anxiety was distinctly associated with neural connectivity between the right amygdala and posterior aspect of the ipsilateral STS. For the orientation component, we observed a significant anxiety-related interaction with amygdala-STS connectivity ($F_{1, 48} = 6.48$, $p = 0.01$; $\eta_p^2 = 0.12$; 95% CI [0.07, 0.57]), which remained significant after controlling for co-morbid depressive symptoms ($r(49) = 0.34$, $p = 0.02$; 95% CI [0.07, 0.56]). Specifically, weaker amygdala-STS connectivity during avoidant orientation was associated with greater social anxiety severity ($r(49) = -0.27$, $p = 0.056$; 95% CI [−0.01, 0.51]; see Fig. 6), which was not observed during vigilant orientation ($r(49) = 0.05$, $p = 0.75$; 95% CI [−0.23, 0.32] see Fig. 8). For the disengagement component, however, no anxiety-related interaction was observed with amygdala-STS connectivity ($F_{1, 48} = 1.80$, $p = 0.19$; $\eta_p^2 = 0.04$).

4. Discussion

By dissociating threat-related attention patterns across individual trials, we observed a notably consistent pattern of *response-based differences* across measures of behavior, neural activation, and neural connectivity, which were not observed using standard computation measures. Based on standard behavioral measures of threat-related attention, no evidence of threat-related orientation or disengagement of attention was observed. In contrast, response-based behavioral measures of threat-related attention all significantly differed

from zero. In terms of absolute magnitude, avoidant orientation was greater than vigilant orientation, whereas slow disengagement was greater than fast disengagement. Mirroring these behavioral findings, response-based differences derived from separate trials were also reflected in both neural activation and neural connectivity. Although we did not observe activation differences within *a priori* regions (amygdala and vlPFC), whole-brain analyses revealed that avoidant orientation and slow disengagement were characterized by greater *de*activation within the mPFC, PCC, and SFG compared to vigilant orientation and fast disengagement, respectively. Similarly, avoidant orientation and slow disengagement were also characterized by greater connectivity between the right amygdala and an occipito-STS cluster compared to vigilant and fast disengagement, respectively. Finally, we observed that weaker neural connectivity between the right amygdala and the occipito-STS cluster during avoidant orientation was associated with greater social anxiety symptoms.

Whereas standard RT measures failed to detect evidence of threat-related orientation or disengagement, significant differences in absolute magnitude and relative frequency were observed between among response-based measures. This pattern of results is consistent with emerging research that suggests anxiety is characterized by *heterogeneous* patterns of threat-related attention, which may masked by standard attention measures (Evans & Britton, 2018; Zvielli et al., 2014a, 2014b). Across the sample, socially anxious individuals exhibited stronger avoidant orientation and slow disengagement relative to vigilant orientation and fast disengagement, respectively. Standard attention measures failed to detect these differences in magnitude given that avoidant orientation and slow disengagement responses were also comparatively less *frequent*.

In social anxiety, avoidant orientation and slow disengagement responses may exhibit inverse patterns of magnitude and frequency due to these attention patterns recruiting top-down processes such as attentional control (Cisler & Koster, 2010). Specifically, the comparatively greater *magnitude* of avoidant orientation and slow disengagement may suggest these responses emerge when threat exerts a particularly demanding influence on attention, which marshals the recruitment of top-down processes. Due to the resource costs required to recruit top-down processes, however, avoidant orientation and slow disengagement may nevertheless occur less *frequently* to economize attentional resources. Neural activation and neural connectivity patterns associated with avoidant orientation and slow disengagement were consistent with this interpretation.

In the current study, avoidant orientation and slow disengagement may recruit top-down processes in response to particularly influential social threats. Avoidant orientation and slow disengagement responses were both associated with greater *de*activation of the PCC, mPFC, and left SFG, which are hubs within the larger DMN (Greicius et al., 2003). Consistent with operating as DMN hubs, exploratory analyses revealed strong coherence in response-based activation among these neural regions. Deactivation of DMN hubs supports the allocation of attentional resources towards processing external stimuli (for a review, see Anticevic et al., 2012). For example, DMN *de*activation occurs when attentional resources are recruited to support top-down processes such as identifying specific stimulus features (Buckner, Andrews-Hanna, & Schacter, 2008; Singh & Fawcett, 2008; Weissman, Roberts, Visscher, & Woldorff, 2006).

Despite similar underlying neural mechanisms, however, avoidant orientation and slow disengagement represent opposing patterns of attention to social threat. Both avoidant orientation and slow disengagement require greater attentional resources, recruit top-down processes, and exhibit greater DMN *de*activation. However, these seemingly paradoxical brain-behavior relationships may be better understood in the context of facilitating distinct functions. Specifically, avoidant orientation is proposed to reduce negative affect associated with threat processing, whereas slow disengagement is proposed to facilitate elaborative processing of threats (Cisler & Koster, 2010; Taylor, Cross, & Amir, 2016). As such, avoidant orientation *decreases* engagement with a social threat, slow disengagement *increases* engagement with a social threat. Despite these distinct functions, however, avoidant orientation and slow disengagement may both require greater attentional resources.

Consistent with this interpretation, avoidant orientation and slow disengagement were also characterized by greater connectivity between the right amygdala and the anatomically heterogenous cluster centered in the posterior aspect of the STS (BA 19). Research suggests that connectivity between the amygdala and posterior STS plays a central role in distributed neural systems that facilitate face processing (Calder & Young, 2005; Haxby, Hoffman, & Gobbini, 2000). Following early visual input, the posterior aspect of the STS serves as an entry point for processing face-related information, which is subsequently projected to the amygdala (Pitcher, Japee, Rauth, & Ungerleider, 2017). Together, these regions play a critical role in detecting and categorizing emotional perception of facial expressions (Adolphs, 2002). In the current study, greater amygdala and posterior STS connectivity underlying avoidant orientation and slow disengagement responses may suggest that these attention patterns facilitate enhanced processing of social threats, albeit for different purposes (Pine, 2003). As noted previously, past research has suggested that avoidant orientation facilitates emotional regulation processes (Cisler & Koster, 2010; Vassilopoulos, 2005). Consistent with a regulatory function, impaired amygdala-STS connectivity during avoidant orientation was associated with greater social anxiety symptoms. Future research will be necessary, however, to delineate the cognitive outcomes associated with each type of threat-related attention.

Although our response-based approach revealed mechanistic insights, response-based RT measures did not demonstrate associations with social anxiety symptoms. We recruited a sub-clinical sample of socially anxious adults who reported a restricted range of social anxiety symptoms. Given this restricted range, anxiety-related associations may be difficult to detect. Sampling across a wider continuum of social anxiety that includes both non-clinical and clinical anxiety may facilitate detection of anxiety-related associations with response-based measures. However, we did observe associations between response-based measures of amygdala connectivity and social anxiety, which provides some evidence of clinical validity.

Moreover, we believe that several findings support the clinical validity of our response-based computation approach despite the lack of observed anxiety-related associations. First, response-based measures revealed a complex interplay between the *magnitude* and *frequency* of attentional processes. Although this interplay was not associated with symptoms at the *individual* level response-based computation more accurately characterized

threat-related attention in at the *group* level. Second, response-based computation revealed patterns of DMN deactivation and amygdala-STS connectivity, which mirrored behavioral response-based measures. Importantly, response-based measures of amygdala-STS connectivity predicted social anxiety symptoms, which provides some evidence for the clinical validity of response-based computation. Nevertheless, future research will be necessary to comprehensively assess the clinical utility of response-based computation.

Given the novelty of our response-based approach, several caveats should be noted and discussed. RTs demonstrate a positively skewed distribution because RTs can theoretically increase infinitely, but inherently cannot decrease below 0 ms. Given this skewed distribution, it could be argued that differences in magnitude among response-based measures may be attributable to the positive skew of RTs. For example, the greater magnitude of avoidant orientation compared to vigilant orientation could be influenced by the positive skew of RTS. We took several steps to mitigate this potential bias, including the implementation of RT outlier cut-offs, non-parametric analyses, and comprehensive analysis of RT distributions across individual participants. Nevertheless, these steps cannot completely eliminate the potential bias of skewed RT distributions. Additionally, response-based computation is a novel approach that remains relatively untested compared to standard computation approaches. In the absence of a mature literature on response-based computation, findings should be cautiously interpreted until further research is conducted.

Several other limitations should be noted. First, this study was conducted in a sub-clinical socially anxious sample without a matching control sample. Future research in individuals ranging from non-anxious to clinically anxious will be necessary to characterize anxiety-related differences in both the behavioral expression and the neural mechanisms underlying threat-related attention patterns. Second, some additional limitations of response-based measures should be noted. By sub-dividing the number of congruent and incongruent trials, response-based computation inherently reduces the number of trials available for analysis. Assuming an equal number of vigilant orientation and avoidance orientation trials, for example, 40 congruent trials would be sub-divided into 20 trials of each response type. Moreover, individuals exhibit distinct distributions of response types, which introduces heterogeneity in the number of fMRI regressors available across participants (Evans & Britton, 2018). To account for this potential heterogeneity, we utilized a mixed modelling approach in AFNI. Nevertheless, a response-based approach inherently introduces inter-individual variability in the number of trials that contribute to each regressor in fMRI models. Finally, the amygdala is not an anatomically or functionally homogenous structure, but is instead comprised of distinct sub-nuclei (Janak & Tye, 2015). Even at a very liberal threshold for small volume correction (SVC; $p > 0.05$, uncorrected), however, we did not observe any significant activation clusters within the left or right amygdala. Although no amygdala activation differences were noted, it is possible that sub-nuclei populations such as the basolateral and centromedial amygdala exhibit divergent patterns of connectivity with other neural structures during various patterns of threat-related attention. Although outside the scope of the current study, characterizing contributions of amygdala sub-nuclei to threat-related attention will be an important step for further research.

Despite these limitations, our collective results converged across behavior, neural activity, and neural connectivity to suggest that threat-related attention patterns modulate processing of social threat cues in social anxiety. Compared to vigilant orientation and fast disengagement, avoidant orientation and slow disengagement were characterized by relatively greater deactivation of several DMN hubs (PCC, mPFC, SFG) and relatively stronger coupling between the right amygdala and posterior STS. Taken together, our results indicate that social anxiety may be characterized by heterogenous expression threat-related attention, which is supported by functionally distinct processes. Notably, this interpretation is consistent with a growing body of research that suggests that the variability of threat-related attention in social anxiety may be attributable to core deficits in top-down processes such as attentional control (Heeren, Mogoase, McNally, Schmitz, & Philippot, 2015; Taylor et al., 2016). Recently, attention training methods have been developed that are designed to reduce the variability of threat-related attention exhibited by clinical populations, which may provide a promising treatment modality in social anxiety (Lazarov et al., 2019). Offering important clinical implications, these results add to a growing body of evidence suggesting that threat-related attention in social anxiety may be more heterogeneous than previously proposed.

Acknowledgements

We would like to thank Gang Chen and Rick Reynolds for their helpful discussions on amplitude modulation in AFNI.

Funding

This research was supported (in part) by the Intramural Research Program of the NIMH (ZIAMH-0027881). Dr. Britton received support from National Institute of Mental Health (K99/R00 MH091183) during the conduct of the study.

References

Adenauer H, Pinosch S, Catani C, Gola H, Keil J, Kisler J, et al. (2010). Early processing of threat cues in posttraumatic stress disorder—evidence for a cortical vigilance-avoidance reaction. Biological Psychiatry, 68(5), 451–458. 10.1016/j.biopsych.2010.05.015. [PubMed: 20619396]

Adolphs R (2002). Recognizing emotion from facial expressions: Psychological and neurological mechanisms. Behavioral and Cognitive Neuroscience Reviews, 1(1), 21–62. 10.1177/1534582302001001003. [PubMed: 17715585]

Amir N, Beard C, Taylor CT, Klumpp H, Elias J, Burns M, et al. (2009). Attention training in individuals with generalized social phobia: A randomized controlled trial. Journal of Consulting and Clinical Psychology, 77(5), 961–973. 10.1037/a0016685. [PubMed: 19803575]

Amir N, Elias J, Klumpp H, & Przeworski A (2003). Attentional bias to threat in social phobia: Facilitated processing of threat or difficulty disengaging attention from threat? Behaviour Research and Therapy, 41(11), 1325–1335. [PubMed: 14527531]

Anticevic A, Cole MW, Murray JD, Corlett PR, Wang X-J, & Krystal JH (2012). The role of default network deactivation in cognition and disease. Trends in Cognitive Sciences, 16(12), 584–592. 10.1016/j.tics.2012.10.008. [PubMed: 23142417]

Baker SL, Heinrichs N, Kim H-J, & Hofmann SG (2002). The liebowitz social anxiety scale as a self-report instrument: A preliminary psychometric analysis. Behaviour Research and Therapy, 40(6), 701–715. 10.1016/S0005-7967(01)00060-2. [PubMed: 12051488]

Bar-Haim Y, Lamy D, Pergamin L, Bakermans-Kranenburg MJ, & van IJzendoorn MH (2007). Threat-related attentional bias in anxious and nonanxious individuals: A meta-analytic study. Psychological Bulletin, 133(1), 1–24. 10.1037/0033-2909.133.1.1. [PubMed: 17201568]

Barry TJ, Vervliet B, & Hermans D (2015). An integrative review of attention biases and their contribution to treatment for anxiety disorders. Frontiers in Psychology, 6(968), 10.3389/fpsyg.2015.00968.

Beck AT, Steer RA, & Brown GK (1996). Manual for the beck depression inventory-ii. San Antonio, TX: Psychological Corporation.

Bishop SJ (2009). Trait anxiety and impoverished prefrontal control of attention. Nature Neuroscience, 12(1), 92–98. 10.1038/nn.2242. [PubMed: 19079249]

Britton JC, Bar-Haim Y, Carver FW, Holroyd T, Norcross MA, Detloff A, et al. (2012). Isolating neural components of threat bias in pediatric anxiety. The Journal of Child Psychology and Psychiatry and Allied Disciplines, 53(6), 678–686. 10.1111/j.1469-7610.2011.02503.x. [PubMed: 22136196]

Britton JC, Suway JG, Clementi MA, Fox NA, Pine DS, & Bar-Haim Y (2015). Neural changes with attention bias modification for anxiety: A randomized trial. Social Cognitive and Affective Neuroscience, 10(7), 913–920. 10.1093/scan/nsu141. [PubMed: 25344944]

Browning M, Holmes EA, Murphy SE, Goodwin GM, & Harmer CJ (2010). Lateral prefrontal cortex mediates the cognitive modification of attentional bias. Biological Psychiatry, 67(10), 919–925. 10.1016/j.biopsych.2009.10.031. [PubMed: 20034617]

Buckner RL, Andrews-Hanna JR, & Schacter DL (2008). The brain's default network: Anatomy, function, and relevance to disease. Annals of the New York Academy of Sciences, 1124, 1–38. 10.1196/annals.1440.011. [PubMed: 18400922]

Calder AJ, & Young AW (2005). Understanding the recognition of facial identity and facial expression. Nature Reviews Neuroscience, 6(8), 641–651. 10.1038/nrn1724. [PubMed: 16062171]

Cisler JM, & Koster EHW (2010). Mechanisms of attentional biases towards threat in the anxiety disorders: An integrative review. Clinical Psychology Review, 30(2), 203. 10.1016/j.cpr.2009.11.003. [PubMed: 20005616]

Cox RW, Chen G, Glen DR, Reynolds RC, & Taylor PA (2017). Fmri clustering and false-positive rates. Proceedings of the National Academy of Sciences, 114(17), E3370–E3371. 10.1073/pnas.1614961114.

El Khoury-Malhame M, Reynaud E, Soriano A, Michael K, Salgado-Pineda P, Zendjidjian X, et al. (2011). Amygdala activity correlates with attentional bias in ptsd. Neuropsychologia, 49(7), 1969–1973. [PubMed: 21440563]

Evans TC, & Britton JC (2018). Improving the psychometric properties of dot-probe attention measures using response-based computation. Journal of Behavior Therapy and Experimental Psychiatry, 60, 95–103. 10.1016/j.jbtep.2018.01.009. [PubMed: 29580549]

Evans TC, Walukevich KA, & Britton JC (2016). Vigilance-avoidance and disengagement are differentially associated with fear and avoidant behaviors in social anxiety. Journal of Affective Disorders, 199, 124–131. 10.1016/j.jad.2016.04.003. [PubMed: 27131063]

Fani N, Jovanovic T, Ely TD, Bradley B, Gutman D, Tone EB, et al. (2012). Neural correlates of attention bias to threat in post-traumatic stress disorder. Biological Psychology, 90(2), 134–142. 10.1016/j.biopsycho.2012.03.001. [PubMed: 22414937]

First MB, Spitzer RL, Gibbon M, & Williams JBW (2002). Structured clinical interview for dsm-iv-tr axis i disorders, research version, patient edition. (scid-i/p). New York: Biometrics Research, New York State Psychiatric Institute.

Greicius MD, Krasnow B, Reiss AL, & Menon V (2003). Functional connectivity in the resting brain: A network analysis of the default mode hypothesis. Proceedings of the National Academy of Sciences, 100(1), 253–258. 10.1073/pnas.0135058100.

Haxby JV, Hoffman EA, & Gobbini MI (2000). The distributed human neural system for face perception. Trends in Cognitive Sciences, 4(6), 223–233. [PubMed: 10827445]

Heeren A, Mogoase C, McNally RJ, Schmitz A, & Philippot P (2015). Does attention bias modification improve attentional control? A double-blind randomized experiment with individuals with social anxiety disorder. Journal of Anxiety Disorders, 29, 35–42. 10.1016/j.janxdis.2014.10.007. [PubMed: 25465885]

Heeren A, Mogoase C, Philippot P, & McNally RJ (2015). Attention bias modification for social anxiety: A systematic review and meta-analysis. Clinical Psychology Review, 40, 76–90. 10.1016/j.cpr.2015.06.001. [PubMed: 26080314]

Heimberg RG, Homer KJ, Juster HR, Safren SA, Brown EJ, Schneier F.r., et al. (1999). Psychometric properties of the liebowitz social anxiety scale. Psychological Medicine, 29(1), 199–212. 10.1017/S0033291798007879. [PubMed: 10077308]

van den Heuvel OA, Veltman DJ, Groenewegen HJ, Witter MP, Merkelbach J, Cath DC, et al. (2005). Disorder-specific neuroanatomical correlates of attentional bias in obsessive-compulsive disorder, panic disorder, and hypochondriasis. Archives of General Psychiatry, 62(8), 922–933. 10.1001/archpsyc.62.8.922. [PubMed: 16061770]

Janak PH, & Tye KM (2015). From circuits to behaviour in the amygdala. Nature, 517(7534), 284–292. 10.1038/nature14188. [PubMed: 25592533]

Kim SH, & Hamann S (2007). Neural correlates of positive and negative emotion regulation. Journal of Cognitive Neuroscience, 19(5), 776–798. 10.1162/jocn.2007.19.5.776. [PubMed: 17488204]

Klumpp H, & Amir N (2009). Examination of vigilance and disengagement of threat in social anxiety with a probe detection task. Anxiety, Stress, and Coping, 22(3), 283–296. 10.1080/10615800802449602. [PubMed: 19253172]

Koster EH, Crombez G, Verschuere B, & De Houwer J (2004). Selective attention to threat in the dot probe paradigm: Differentiating vigilance and difficulty to disengage. Behaviour Research and Therapy, 42(10), 1183–1192. 10.1016/j.brat.2003.08.001. [PubMed: 15350857]

Lazarov A, Suarez-Jimenez B, Abend R, Naim R, Shvil E, Helpman L, et al. (2019). Bias-contingent attention bias modification and attention control training in treatment of ptsd: A randomized control trial. Psychological Medicine, 49(14), 2432–2440. 10.1017/S0033291718003367. [PubMed: 30415648]

Liebowitz MR (1987). Social phobia. Modern Problems of Pharmacopsychiatry, 22, 141–173. [PubMed: 2885745]

Mansell W, Clark DM, Ehlers A, & Chen Y-P (1999). Social anxiety and attention away from emotional faces. Cognition & Emotion, 13(6), 673–690. 10.1080/026999399379032.

McLaren DG, Ries ML, Xu G, & Johnson SC (2012). A generalized form of context-dependent psychophysiological interactions (gppi): A comparison to standard approaches. NeuroImage, 61(4), 1277–1286. 10.1016/j.neuroimage.2012.03.068. [PubMed: 22484411]

Mogg K, & Bradley BP (2016). Anxiety and attention to threat: Cognitive mechanisms and treatment with attention bias modification. Behaviour Research and Therapy, 87, 76–108. 10.1016/j.brat.2016.08.001. [PubMed: 27616718]

Monk CS, Telzer EH, Mogg K, Bradley BP, Mai X, Louro HMC, et al. (2008). Amygdala and ventrolateral prefrontal cortex activation to masked angry faces in children and adolescents with generalized anxiety disorder. Archives of General Psychiatry, 65(5), 568–576. 10.1001/archpsyc.65.5.568. [PubMed: 18458208]

Pine DS (2003). Developmental psychobiology and response to threats: Relevance to trauma in children and adolescents. Biological Psychiatry, 53(9), 796–808. 10.1016/S0006-3223(03)00112-4. [PubMed: 12725972]

Pineles SL, & Mineka S (2005). Attentional biases to internal and external sources of potential threat in social anxiety. Journal of Abnormal Psychology, 114(2), 314–318. 10.1037/0021-843x.114.2.314. [PubMed: 15869362]

Pitcher D, Japee S, Rauth L, & Ungerleider LG (2017). The superior temporal sulcus is causally connected to the amygdala: A combined tbs-fmri study. Journal of Neuroscience, 37(5), 1156–1161. 10.1523/jneurosci.0114-16.2016. [PubMed: 28011742]

Price M, Tone EB, & Anderson PL (2011). Vigilant and avoidant attention biases as predictors of response to cognitive behavioral therapy for social phobia. Depression and Anxiety, 28(4), 349–353. 10.1002/da.20791. [PubMed: 21308888]

Rytwinski NK, Fresco DM, Heimberg RG, Coles ME, Liebowitz MR, Cissell S, et al. (2009). Screening for social anxiety disorder with the self-report version of the liebowitz social anxiety scale. Depression and Anxiety, 26(1), 34–38. 10.1002/da.20503. [PubMed: 18781659]

Singh KD, & Fawcett IP (2008). Transient and linearly graded deactivation of the human default-mode network by a visual detection task. NeuroImage, 41(1), 100–112. 10.1016/j.neuroimage.2008.01.051. [PubMed: 18375149]

Taylor CT, Aupperle RL, Flagan T, Simmons AN, Amir N, Stein MB, et al. (2014). Neural correlates of a computerized attention modification program in anxious subjects. Social Cognitive and Affective Neuroscience, 9(9), 1379–1387. 10.1093/scan/nst128. [PubMed: 23934417]

Taylor CT, Cross K, & Amir N (2016). Attentional control moderates the relationship between social anxiety symptoms and attentional disengagement from threatening information. Journal of Behavior Therapy and Experimental Psychiatry, 50, 68–76. 10.1016/j.jbtep.2015.05.008. [PubMed: 26072705]

Vassilopoulos SP (2005). Social anxiety and the vigilance-avoidance pattern of attentional processing. Behavioural and Cognitive Psychotherapy, 33(1), 13–24. 10.1017/S1352465804001730.

Wechsler D (1999). Wechsler abbreviated scale of intelligence (wasi). San Antonio, TX: Harcourt Assessment, Inc.

Weissman DH, Roberts KC, Visscher KM, & Woldorff MG (2006). The neural bases of momentary lapses in attention. Nature Neuroscience, 9, 971. 10.1038/nn1727. [PubMed: 16767087]

Yiend J, Mathews A, Burns T, Dutton K, Fernandez-Martin A, Georgiou GA, et al. (2015). Mechanisms of selective attention in generalized anxiety disorder. Clinical psychological science : A Journal of the Association for Psychological Science, 3(5), 758–771. 10.1177/2167702614545216. [PubMed: 26504675]

Zvielli A, Bernstein A, & Koster EHW (2014a). Dynamics of attentional bias to threat in anxious adults: Bias towards and/or away? PloS One, 9(8), Article e104025. 10.1371/journal.pone.0104025. [PubMed: 25093664]

Zvielli A, Bernstein A, & Koster EHW (2014b). Temporal dynamics of attentional bias. Clinical Psychological Science. 10.1177/2167702614551572.

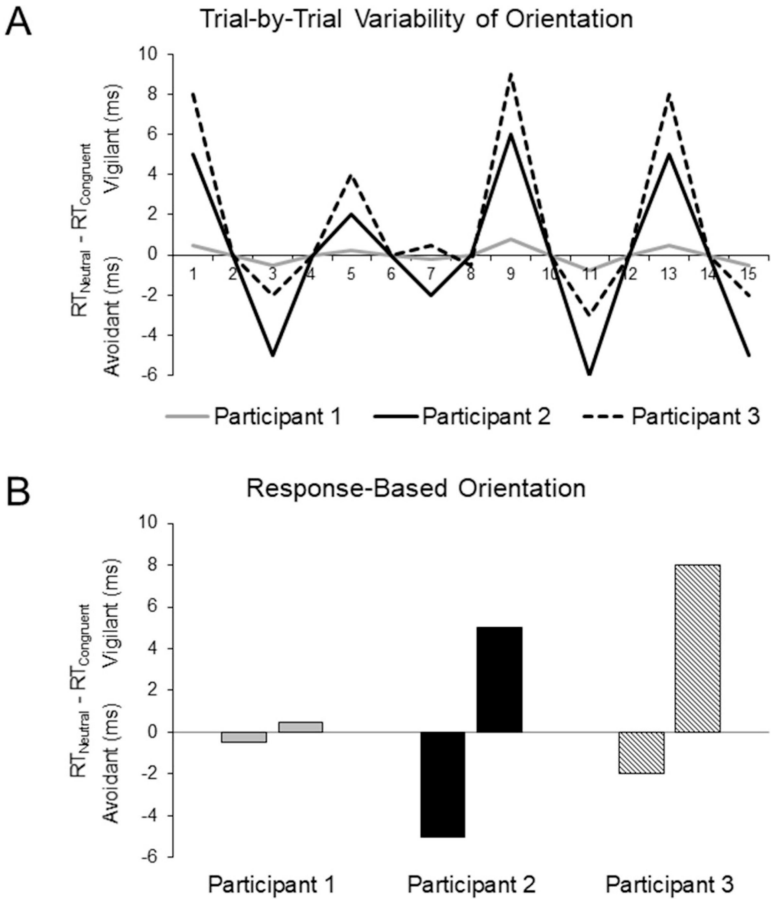

Fig. 1. Hypothetical Individual Differences in Threat-Related Orientation of Attention.

A). Hypothetical distributions of response patterns within the dot-probe task. When congruent reaction time (RT) is referenced against mean neutral RT ($RT_{Neutral} - RT_{Congruent}$), positive and negative scores indicate vigilant and avoidant orientation, respectively. Utilizing standard computation approaches, both Participant 1 and Participant 2 exhibit distributions of orientation scores that would produce a standard orientation score of 0 ms, although Participant 2 exhibits significant vigilant and avoidant orientation of equal magnitude. Participant 3 exhibits a general pattern of vigilant orientation, generated by a disproportionate vigilant vs. avoidant orientation. B). However, utilizing a response-based computation approach accurately captures co-occurring patterns of vigilant and avoidant orientation at varying degrees of magnitude. *Reference:* Reprinted from *Journal of Behavioral and Experimental Psychiatry,* Evans, T. C., & Britton, J. C., Improving the psychometric properties of dot-probe attention measures using response-based computation, Copyright (2018), with permission from Elsevier.

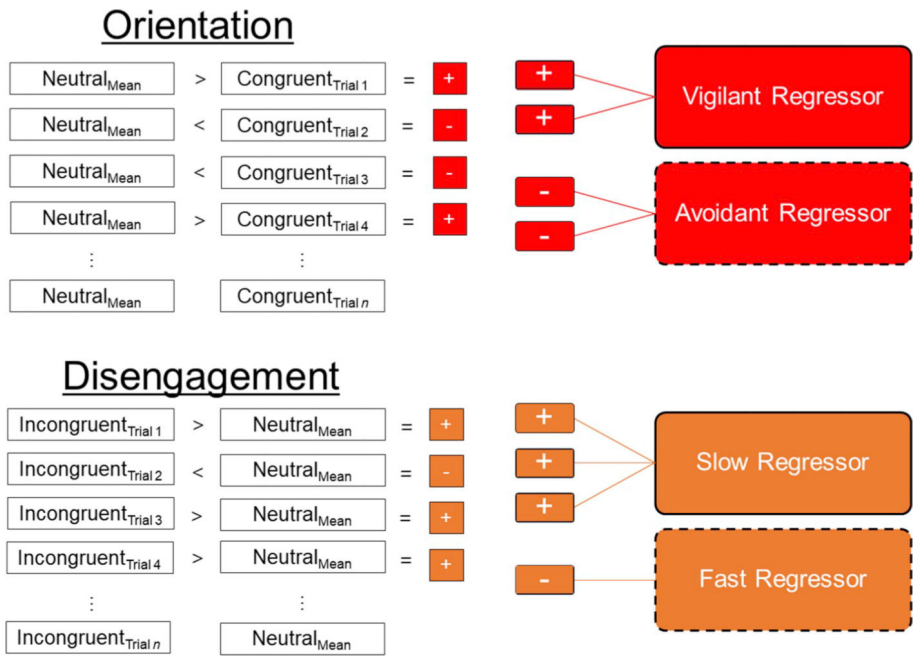

Fig. 2. Response-Based Generation of Individual-Level fMRI Models.

Using a response-based approach to computing threat-related attention, individual congruent and incongruent trials from each participant were separately referenced to that participant's mean neutral reaction time (e.g., $RT_{NeutralMean} - RT_{Congruent}$ [Trial 1 … Trial 2 … Trial *n*]). For individual congruent trials, positive responses were coded as vigilant orientation trials, whereas negative responses were coded as avoidant orientation trials. For incongruent trials, negative responses were coded as fast disengagement trials, whereas positive responses were coded as slow disengagement trials. Regressors were subsequently computed for each individual according to their respective distribution of responses (vigilant orientation, avoidant orientation, slow disengagement, fast disengagement).

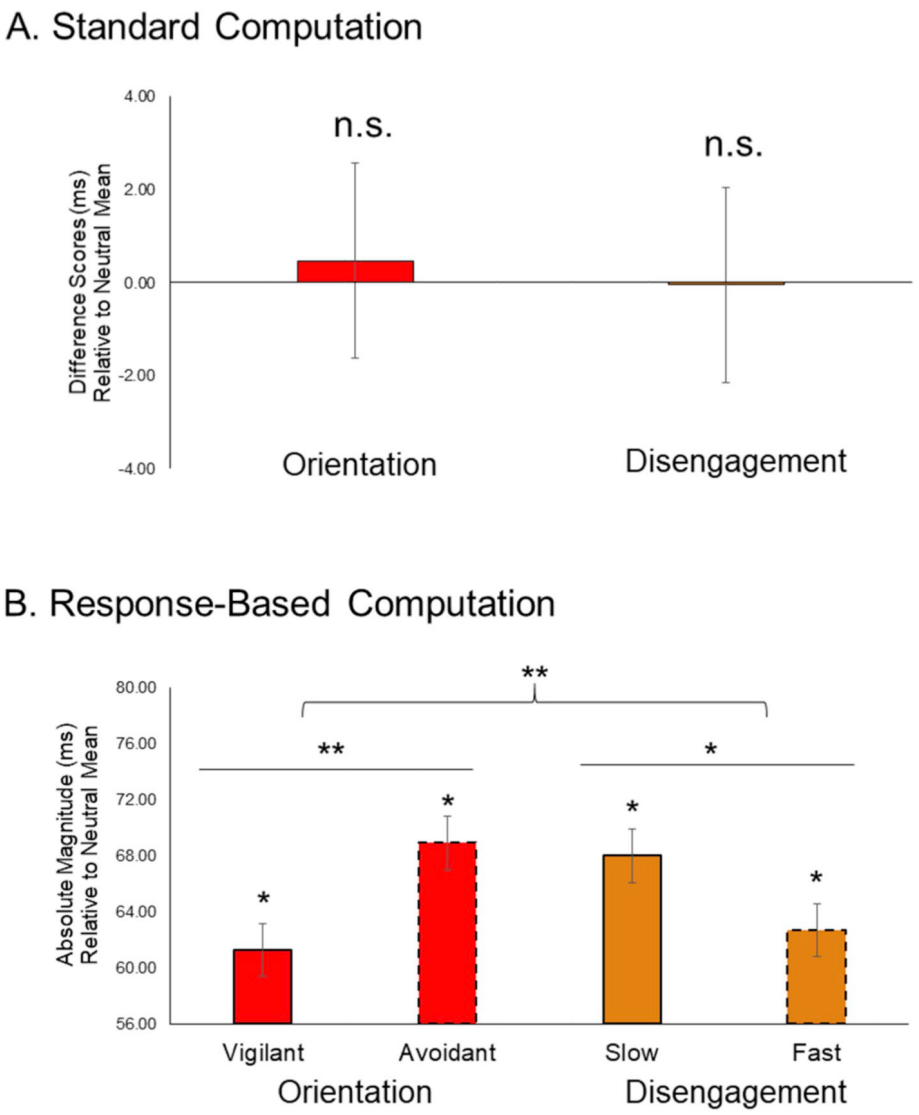

Fig. 3. Comparing Standard and Response-Based Measures of Threat-Related Attention.

A). Using standard computation, no evidence of threat-related orientation ($RT_{NeutralMean} - RT_{CongruentMean}$) or disengagement ($RT_{IncongruentMean} - RT_{NeutralMean}$) was observed. B). Using response-based computation, a significant Attention Type (Orientation vs. Disengagement) × Attention Direction (Positive vs. Negative) interaction was observed ($p = 0.004$). Within the orientation component, avoidant orientation was greater in absolute magnitude compared to vigilant orientation ($p = 0.007$). Within the disengagement component, slow disengagement was greater in absolute magnitude compared to fast disengagement ($p = 0.05$). * = $p < 0.05$.

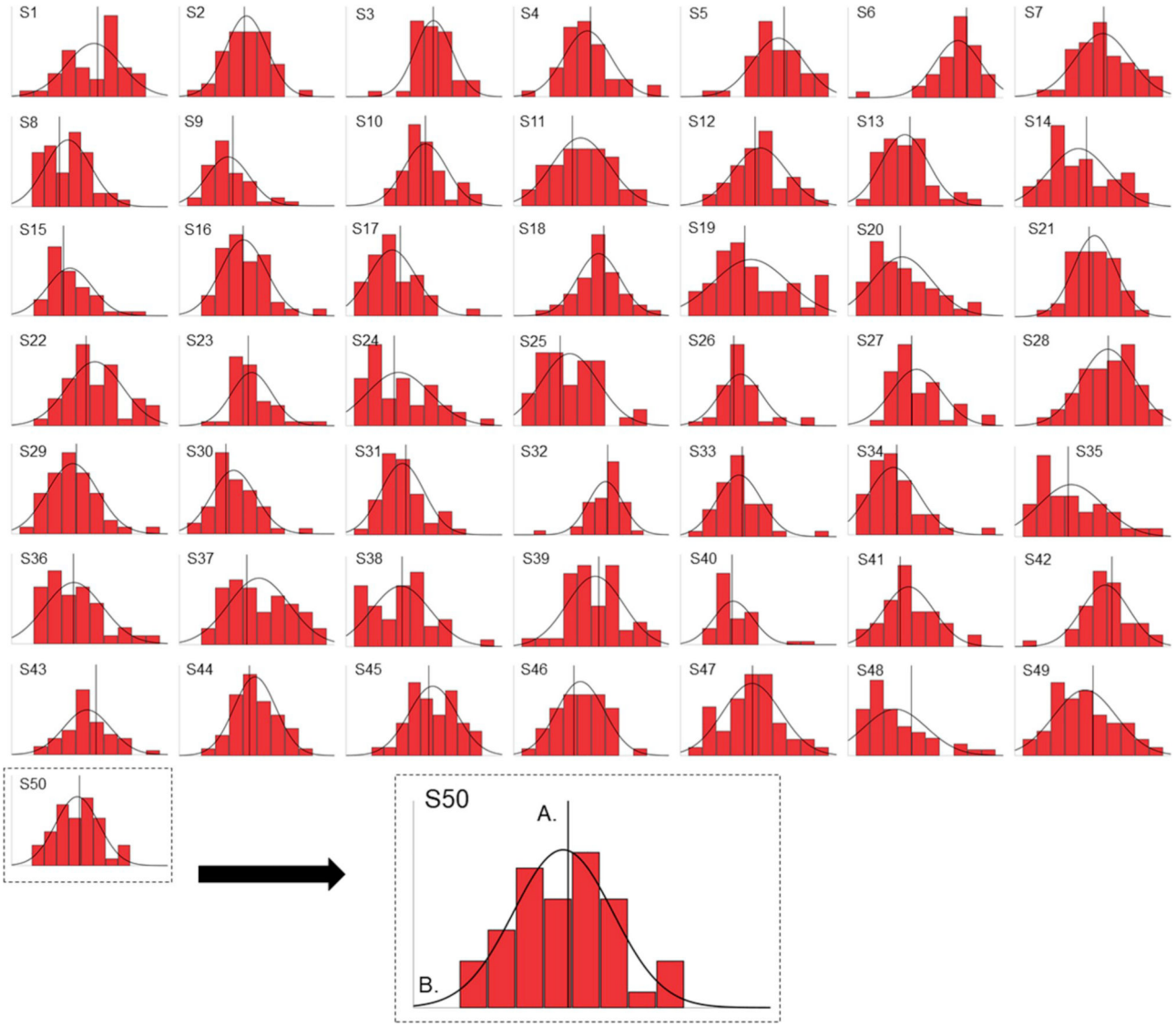

Fig. 4. Subject-Level Distributions of Congruent Reaction Times

Frequency distributions of congruent reaction times (blue) are plotted separately for each of the 50 subjects included in final analyses (S1 – S50). A). Reference line on the x-axis denotes the unique mean of neutral-neutral trials, which is computed separately for each subject. B). Normal distribution curves are depicted separately based each subject's unique congruent reaction time distribution. (For interpretation of the references to colour in this figure legend, the reader is referred to the Web version of this article.)

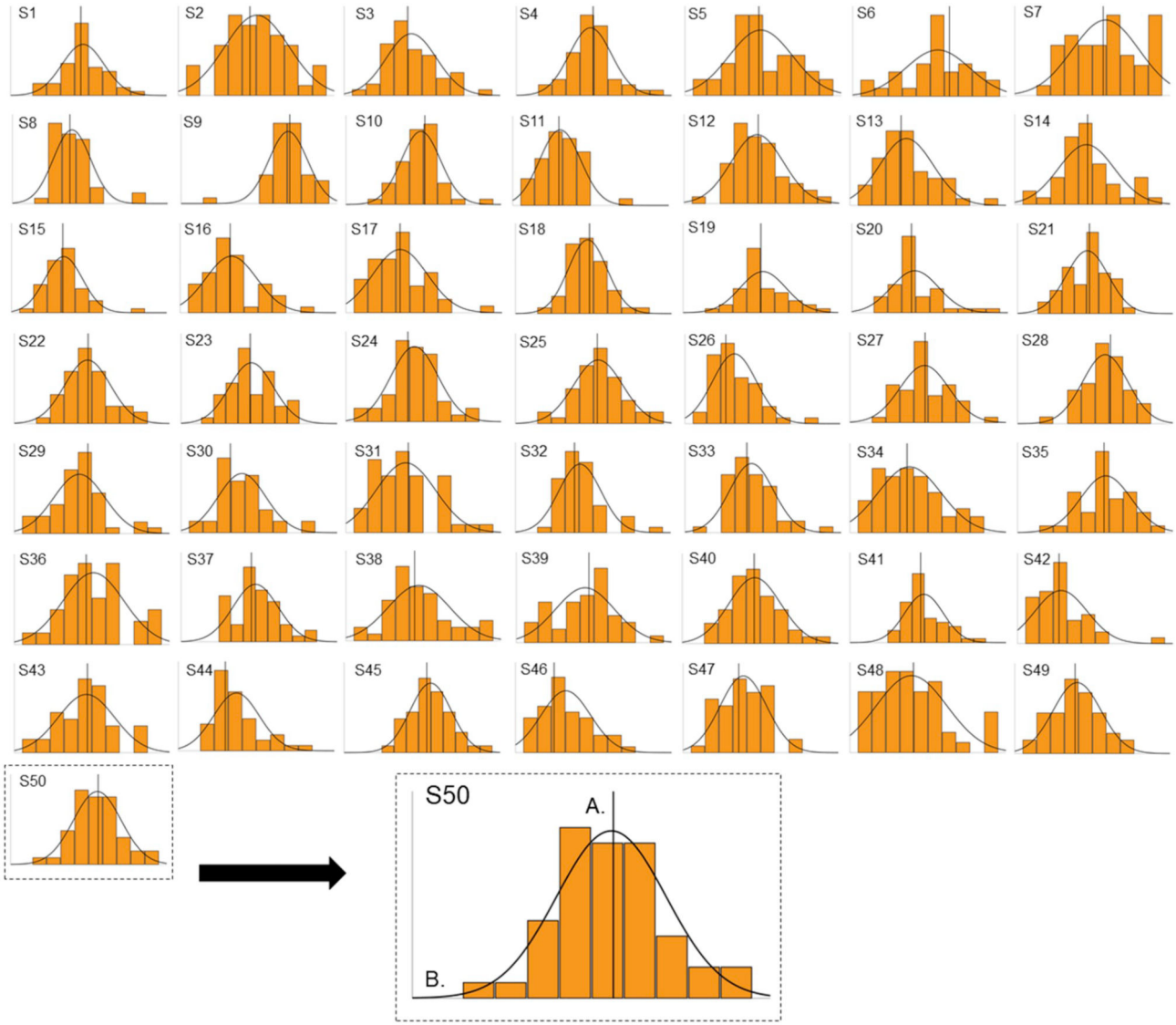

Fig. 5. Subject-Level Distributions of Incongruent Reaction Times.

Frequency distributions of incongruent reaction times (red) are plotted separately for each of the 50 subjects included in final analyses (S1 – S50). A). Reference line on the x-axis denotes the unique mean of neutral-neutral trials, which is computed separately for each subject. B). Normal distribution curves are depicted separately based each subject's unique incongruent reaction time distribution. (For interpretation of the references to colour in this figure legend, the reader is referred to the Web version of this article.)

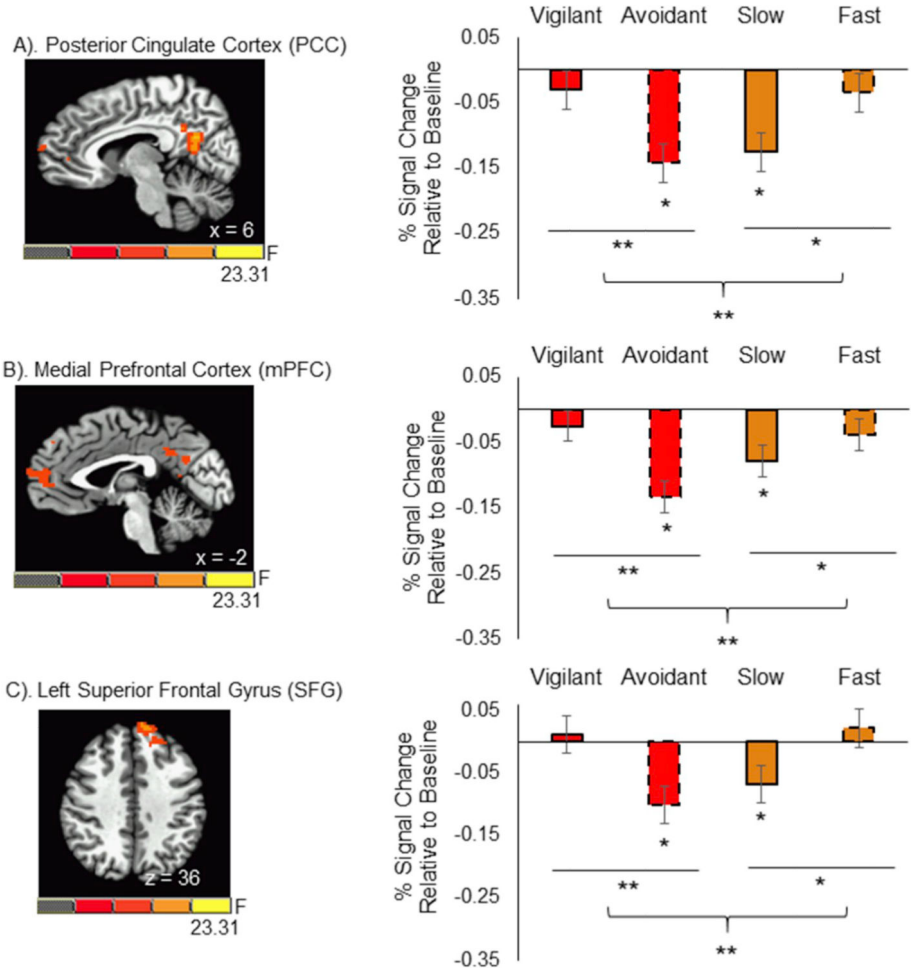

Fig. 6. Response-Based Differences in Neural Deactivation between Orientation and Disengagement.

Response-based differences in neural deactivation were observed within the Posterior cingulate cortex (PCC), medial prefrontal cortex (mPFC), and left superior frontal gyrus (SFG). Across these three regions, greater deactivation was observed during avoidant orientation compared to vigilant orientation (all p's < 0.007) and during slow disengagement compared to fast disengagement (all p's < 0.04). Avoidant orientation and slow disengagement were characterized by significant deactivation relative to baseline (all p's < 0.01). In contrast, neural activation during vigilant orientation and fast disengagement did not differ significantly from zero (all p's > 0.28). * = $p < 0.05$.

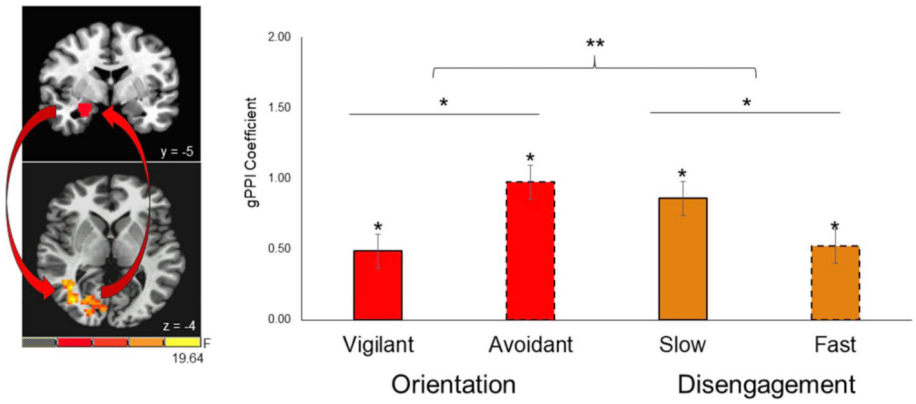

Fig. 7. Response-Based Differences in Amygdala-STS Connectivity Between Orientation and Disengagement.

Response-based differences in neural connectivity were observed between the right amygdala and an anatomically heterogeneous cluster spanning the occipital cortex and posterior aspects of the right superior temporal sulcus (occipito-STS). Stronger connectivity between the right amygdala and the occipito-STS cluster was observed during avoidant orientation compared to vigilant orientation ($p = 0.002$) and during slow disengagement compared to fast disengagement ($p = 0.007$). * = $p < 0.05$.

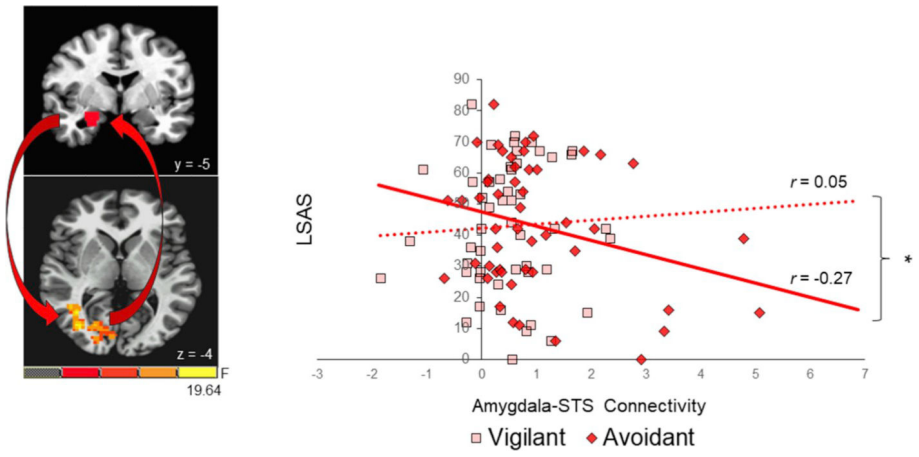

Fig. 8. Social Anxiety is Differentially Associated with Amygdala-STS Connectivity during Vigilant and Avoidant Orientation to Threat.

Based on Liebowitz Social Anxiety Scale (LSAS) scores (Liebowitz, 1987), social anxiety symptoms were associated with neural connectivity between the right amygdala and posterior aspect of the superior temporal sulcus (STS) during orientation of attention to threat ($p = 0.01$). Less amygdala-STS connectivity during avoidant orientation was associated with greater social anxiety severity ($r(49) = -0.27$, $p = 0.056$, dotted red line), whereas amygdala-STS connectivity during vigilant orientation was not associated with social anxiety severity ($r(49) = 0.05$, $p = 0.75$, solid red line). * = $p < 0.05$. (For interpretation of the references to colour in this figure legend, the reader is referred to the Web version of this article.)